The Metal-free and Calcium-bound Structures of a γ-Carboxyglutamic Acid-containing Contryphan from Conus marmoreus , Glacontryphan-M

THE JOURNAL OF BIOLOGICAL CHEMISTRY
Vol. 279, No. 31, Issue of July 30, pp. 32464–32473, 2004

Printed in U.S.A.

The Metal-free and Calcium-bound Structures of a γ-Carboxyglutamic Acid-containing Contryphan from *Conus marmoreus*, Glacontryphan-M*

Received for publication, December 17, 2003, and in revised form, May 18, 2004
Published, JBC Papers in Press, May 20, 2004, DOI 10.1074/jbc.M313826200

Marianne A. Grant‡, Karin Hansson§, Barbara C. Furie‡¶, Bruce Furie‡¶, Johan Stenflo§¶, and Alan C. Rigby‡¶‖

From the ‡Center for Hemostasis, Thrombosis, and Vascular Biology, Beth Israel Deaconess Medical Center and Department of Medicine, Harvard Medical School, Boston, Massachusetts 02215, the §Department of Clinical Chemistry, Lund University, University Hospital, Malmö, Sweden S-205 02, and the ¶Marine Biological Laboratory, Woods Hole, Massachusetts 02543

Glacontryphan-M, a novel calcium-dependent inhibitor of L-type voltage-gated Ca^{2+} channels expressed in mouse pancreatic β-cells, was recently isolated from the venom of the cone snail *Conus marmoreus* (Hansson, K., Ma, X., Eliasson, L., Czerwiec, E., Furie, B., Furie, B. C., Rorsman, P., and Stenflo, J. (2004) *J. Biol. Chem.* 278, 32453–32463). The conserved disulfide-bonded loop of the contryphan family of conotoxins including a D-Trp is present; however, unique to glacontryphan-M is a histidine within the intercysteine-loop and two γ-carboxyglutamic acid (Gla) residues, formed by post-translational modification of glutamic acid. The two calcium-binding Gla residues are located in a four residue N-terminal extension of this contryphan. To better understand the structural and functional significance of these residues, we have determined the structure of glacontryphan-M using two-dimensional ^1H NMR spectroscopy in the absence and presence of calcium. Comparisons of the glacontryphan-M structures reveal that calcium binding induces structural perturbations within the Gla-containing N terminus and the Cys^{11}-Cys^5-Pro^6 region of the intercysteine loop. The backbone of N-terminal residues perturbed by calcium, Gla^2 and Ser^3, moves away from the His^8 and Trp^{10} aromatic rings and the alignment of the D-Trp^7 and His^8 aromatic rings with respect to the Trp^{10} rings is altered. The blockage of L-type voltage-gated Ca^{2+} channel currents by glacontryphan-M requires calcium binding to N-terminal Gla residues, where presumably histidine and tryptophan may be accessible for interaction with the channel. The backbone Cα conformation of the intercysteine loop of calcium-bound glacontryphan-M superimposes on known structures of contryphan-R and Vn (0.83 and 0.66 Å, respectively). Taken together these data identify that glacontryphan-M possesses the canonical contryphan intercysteine loop structure, yet possesses critical determinants necessary for a calcium-induced functionally required conformation.

Venomous marine snails belonging to the genus *Conus* synthesize neuropharmacologically active peptides, conotoxins, which demonstrate unique functional properties for use in prey envenomation and self-defense mechanisms. Conotoxins behave as antagonists, exhibiting molecular specificity for receptor isoforms and ion channels in the neuromuscular system. Most conotoxins appear to be derived from a few gene superfamilies, each distinguished by conserved signal and precursor sequence elements (1). The hallmark of these conotoxins is their conformationally constrained structure, often created through disulfide bridges. These conserved structural scaffolds provide a framework for the presentation of intervening hypervariable regions comprised of post-translationally modified amino acids that contribute to molecular specificity.

Conotoxins of the contryphan family have been found with post-translational modifications including proline hydroxylation, C-terminal amidation, tryptophan bromination (2), and leucine and tryptophan epimerization (3, 4). The nine contryphans characterized to date share the conserved sequence motif, CP*(D-W or D-L)*X*PWC, that includes a tryptophan or leucine in the D-conformation, a disulfide bond between the two cysteines, and in some cases hydroxylation of the proline preceding the D-Trp residue, Pro*. The N-terminal Cys-Pro peptide bond exhibits *cis-trans* isomerization in the contryphans characterized to date; however, the more abundant *cis* isomer is believed to be the functionally relevant conformer (5). The contryphan motif CP*(D-W or L)*X*PWC is a robust structural scaffold, that maintains the backbone structure and α-β bond vector orientation independent of the amino acid that is substituted at residue *X* (6). This residue is Gln in contryphan-Sm (5), Glu in contryphan-R (7), and Lys in contryphan-Vn (8). Functionally, the contryphans elicit a stiff tail syndrome in mice when injected intracranially, or a body tremor and mucous secretion when injected intramuscularly into fish (9). Recently, contryphan-Vn from *Conus ventricosus* has been shown to affect both voltage-gated and Ca^{2+}-dependent potassium channels (K^+ channels) (10), identifying the first functional target for a contryphan.

In the accompanying article (11) we describe the purification, primary structure, and functional characterization of a novel contryphan from the venom of *Conus marmoreous*, glacontryphan-M (11). Glacontryphan-M, with the sequence NγSγCP(D-W)HPWC-NH_2 (γ-carboxyglutamic acid (Gla)[1] residue; NH_2, C-terminal amidation), is the first contryphan found to contain

* This work was supported by the National Science Foundation (to A. C. R.), the National Institutes of Health (to B. F. and B. C. F.) and grants from the Swedish Medical Research Council, the European Union Con-Euro-Pain, and the Swedish Foundation for Strategic Research (to J. S.). The costs of publication of this article were defrayed in part by the payment of page charges. This article must therefore be hereby marked "*advertisement*" in accordance with 18 U.S.C. Section 1734 solely to indicate this fact.

‖ To whom correspondence should be addressed: Center for Hemostasis, Thrombosis, and Vascular Biology, Beth Israel Deaconess Medical Center and Department of Medicine, Harvard Medical School, 330 Brookline Ave., Boston, MA, 02215. Tel.: 617-667-0637; Fax: 617-975-5505; E-mail: arigby@bidmc.harvard.edu.

[1] The abbreviations used are: Gla, γ-carboxyglutamic acid; TOCSY, total correlation spectroscopy; NOESY, nuclear Overhauser enhancement spectroscopy; RMSD, root mean-squared deviation.

Gla, a post-translationally modified glutamic acid residue (Table I). The malonate-like side chain of Gla can chelate divalent metal ions to support metal ion-dependent structural determinants that are critical for function.

To date many Gla-containing conotoxins have been identified and characterized (12–14). The best studied Gla-containing conotoxin is conanotokin-G, a 17-residue neuroactive peptide from *Conus geographus* containing five Gla residues, which antagonizes specific isoforms of the *N*-methyl-D-aspartate (NMDA) receptor (12). The metal binding properties and three-dimensional structure of conantokin-G suggest a structural role for Gla, whereby calcium ion binding by Gla residues increases the α-helicity and structural rigidity of the conantokin (16–18). Another protein family rich in Gla and functionally dependent on divalent metal ion interactions is the vitamin K-dependent protein family, including factor IX, factor VII, prothrombin, and factor X that participate in blood coagulation in vertebrates (Refs. 19 and 20 and references therein). It is well established that the vitamin K-dependent proteins bind to negatively charged phospholipids through a mechanism involving the N-terminal Gla domain (21–23). Nine to twelve Gla residues in this domain (of 45–47 residues in total) facilitate interactions with an array of calcium ions to stabilize a conformation that is required for binding to phospholipid membranes. Apart from the conantokin and vitamin K-dependent protein families, the functional role of Gla is still largely unknown.

Here we report the three-dimensional structure of glacontryphan-M, in the absence and presence of calcium using two-dimensional ^{1}H NMR spectroscopy. Calcium ion binding induces perturbations of the N-terminal residues Gla^2, Ser^3, and Gla^4, and the Cys^{11}-Cys^5-Pro^6 region of the intercysteine loop, resulting in an increased exposure and slight reorientation of the stacked aromatic rings of His^8 and D-Trp^7 relative to the positioning of Trp^{10}. Considering that glacontryphan-M is a calcium-dependent antagonist for L-type voltage-gated Ca^{2+} channels expressed in mouse pancreatic β-cells (11), it is possible that this structural perturbation is necessary for glacontryphan-M to interact with the Ca^{2+} channel in a conformation that expresses a pharmacophore similar to known L-type Ca^{2+} channel antagonists. The elucidation of these molecular determinants will help us to better understand the functional role of Gla within glacontryphan-M and may shed light into the potential interactions that underlie the L-type Ca^{2+} channel antagonism exhibited by this unique conotoxin. A complete understanding of the pharmacological activity that is attributed to the triad of hydrophobic residues, D-Trp^7, His^8, and Trp^{10}, in glacontryphan-M could lead to the development of novel neuropharmacological reagents.

EXPERIMENTAL PROCEDURES

Peptide Synthesis—Glacontryphan-M and the glutamic acid-containing analogue, glucontryphan-M, were synthesized as described by Hansson *et al.* (11). The masses of the peptides were confirmed by Nano-Electro Spray Ionization (NanoESI)-mass spectrometry on an API QSTAR Pulsar-I quadrapole TOF mass spectrometer (Applied Biosystems/MDS Sciex, Toronto, Canada), and the peptides were sequenced by amino acid sequencing as described previously (11).

Circular Dichroism—Lyophilized glacontryphan-M was dissolved in H_2O to a final concentration of 0.2 mM. Samples were adjusted to either pH 5.8 or 7.0 and treated with Chelex resin (Bio-Rad) to remove contaminant metal ions. For calcium binding studies, $CaCl_2$ was titrated into the samples to a final concentration of 6 mM. The CD spectra were collected on a JASCO 810 spectropolarimeter (Jasco Inc., Easton, MD) equipped with a thermoelectric temperature control unit. The spectrometer was calibrated using a standard of D-(+)-10-camphor sulfonic acid. The spectra presented are the average of three wavelength scans between 230 and 340 nm using a pathlength of 1.0 cm, a dwell time of 3 s/nm and at a temperature of 25 °C. All spectra were corrected for light scatter by buffer subtraction. Results are expressed in terms of units of absorption (uA) (24).

Three-dimensional Structure Determination of Glacontryphan-M—Proton assignments were determined from two-dimensional ^{1}H NMR data recorded over a temperature range from 5 to 25 °C on a 500 MHz Varian Unity INOVA spectrometer with a proton frequency of 499.695 MHz. The three-dimensional structures of metal-free and calcium-bound glacontryphan-M were determined from data collected at 9 °C. Samples contained 3 mM synthetic glacontryphan-M peptide in 90% H_2O:10% D_2O, pH 5.8 or 7.0. The carrier frequency was set to the water resonance, which was suppressed using presaturation during the pre-acquisition delay.

Two-dimensional nuclear Overhauser enhancement spectroscopy (NOESY) spectra were recorded with mixing times of 300, 350, and 400 ms at 9 °C. A total of 4096 real data points were acquired in t_2 and 256 time-proportional phase increments (TPPI) were implemented in t_1 with a spectral width of 8000 Hz in the F_2 dimension. A total of 128 summed transients were collected with a relaxation delay of 1.12 s. Additional NOESY data were acquired with relyophilized samples of glacontryphan-M that were reconstituted in 99.996% D_2O (Cambridge Isotope Laboratories, Andover, MA) at a noncorrected pH of 5.8 in order to complete the assignments of resonances located near the water peak and to detect weak NOE cross-peaks. Two-dimensional TOCSY spectra were recorded with a mixing time of 45 ms at 9 °C using the MLEV-17 spin-lock sequence (25). A total of 4096 real data points were acquired in t_2 and 256 TPPI implemented in t_1 with a spectral width of 8000 Hz in the F_2 dimension. A total of 192 summed transients were collected with a relaxation delay of 1.12 s. Spectra were processed with Gaussian and sine bell functions for apodization in t_2 and a shifted sine bell function in t_1 using the VNMR software processing (Varian, Inc., Palo Alto, CA). All data were zero filled to 4K by 4K real matrices. A two-dimensional DQF-COSY spectrum was acquired with 4096 real data points in t_2 and 640 TPPI were implemented in t_1 with a spectral width of 8000 Hz in the F_2 dimension. A total of 96 summed transients were collected for measurement of $^3J_{HN\alpha}$ spin-spin coupling constants in order to derive dihedral torsion angles. A natural abundance ^{1}H-^{13}C heteronuclear single quantum coherence spectrum (HSQC) was acquired with 1024 real data points in t_2 and 160 time proportional phase increments (TPPI) were implemented in t_1 with a spectral width of 17591 Hz in the F_1 dimension and 8000 Hz in the F_2 dimension.

Proton Resonance Assignments—Spin-system identifications of glacontryphan-M proton resonances in the absence of calcium and in the presence of calcium (15 molar equivalents) were completed using a combination DFQ-COSY and TOCSY experiments, which provided ^{1}H-^{1}H through-bond connectivities. For sequence-specific assignments, sequential $d_{\alpha N}$, $d_{\beta N}$, and d_{NN} NOE connectivities were obtained from NOESY experiments. The vicinal spin-spin coupling constants, $^3J_{HN\alpha}$, which were less than 6.2 Hz or greater than 8.0 Hz were used to calculate backbone ϕ torsion angles (26). NOE cross-peak intensities were classified as strong, medium, or weak and converted to distance restraint upper bounds of 2.5, 3.5, and 6.0 Å, respectively (27). Scalar reference peaks were chosen from non-overlapped NH-αH NOE peaks and set to 2.8 Å distances for calibration of the entire set of distance restraints (28). Where possible rotamers of χ^1 angles were categorized as either 60°, 180°, or −60° using qualitative analysis β-proton three-bond coupling ($^3J_{H\alpha\beta^*}$) and NOE intensities, $d_{\alpha\beta1}$, $d_{\alpha\beta2}$, $d_{N\beta1}$, and $d_{N\beta2}$ (27). Non-stereospecifically assigned atoms were treated as pseudoatoms and assigned correction distances (28). A ^{1}H-^{13}C heteronuclear single quantum coherence spectrum (HSQC) was recorded to determine the prolyl peptide bond conformations using the difference in their respective Cβ and Cγ chemical shifts (29, 30). In addition, all of the ^{1}H-^{13}C resonances were assigned to verify the backbone and side chain proton assignments and to resolve ambiguities in assignment of the D-Trp^7, His^8, and Trp^{10} aromatic side chain proton chemical shifts arising from chemical shift degeneracy in the proton dimension.

Structure Calculations—The three-dimensional structure of metal-free glacontryphan-M was determined from a total of 339 distance restraints (142 intraresidue, 197 interresidue; 116 sequential, 51 medium range, and 30 long range) and 30 torsion angle restraints, which were entered into the distance geometry program, DGII (CVFF force field parameters) of InsightII (Accelrys, San Diego, CA) to generate a family of 50 structures using a combination of simulated annealing and distance geometry (31). In the starting structure for molecular dynamics simulation the Cys^5-Pro^6 peptide bond was created in the *cis* conformation and the ω angle was fixed at 0° ± 10°, all other peptide bonds were created in the *trans* conformation. The first family of determined structures showed convergence of the orientation of the angle around the disulfide S-S bond, χ^3. Greater than 80% of the convergent struc-

TABLE 1
Comparison of the sequences of contryphans with known NMR structures

Conopeptide	Amino acid sequence[a,b]	Species	Ref.
Contryphan-R	GCOW**E**PWC-NH_2	*C. radiatus*	Jiminez *et al.,* 1996
Contryphan-Sm	COW**Q**PWC-NH_2	*C. stercusmuscarum*	Jacobsen *et al.,* 1998
Contryphan-Vn	GDCPW**K**PWC-NH_2	*C. ventricosus*	Massilia *et al.,* 2001
Glacontryphan-M	NγSγCPW**H**PWC-NH_2	*C. marmoreus*	Hansson *et al.,* 2004

[a] O, 4-trans-hydroxyproline; W, D-tryptophan, γ, gamma-carboxyglutamic acid.
[b] The hypervariable residue within the intercysteine-loop is in bold.

tures contained the right-handed disulfide bond conformation with a χ^3 angle of approximately +60° (32). These data permitted the addition of distance restraints between the cysteine α-carbons and between the β-carbon of one cysteine and the sulfur atom of the other to the restraint file (32). The 35 conformations with the lowest restraint energy violations were used to represent the structure and the average structure for the ensemble was determined using the Analysis program of InsightII. Average root mean-squared deviation (RMSD) values following superimposition of the backbone heavy atoms of each structure with the geometric average reflected the quality of the determined family of structures.

The structure determination of glacontryphan-M in the presence of 15 molar equivalents of calcium was determined in a manner similar to the methodology described above for the metal-free structure. The three-dimensional structure of calcium-bound glacontryphan-M was determined from a total of 288 distance restraints (135 intraresidue, 153 interresidue; 89 sequential, 46 medium range, and 18 long range) and 12 torsion angle restraints. Greater than 90% of the first family of determined structures showed convergence of the disulfide S-S bond orientation, χ^3, therefore, we restrained the disulfide in the right-handed conformation as described above with a χ^3 of approximately +60° (32). Based on the finding that glacontryphan-M expresses a single, saturable calcium-binding site (K_D 0.63 mM) (11), the final structure calculations included six distance restraints between the Cβ, the Cγ, the Cδ1 and C1 carbons of Gla^2 and Gla^4, to model a bound calcium ion between Gla^2 and Gla^4. These distance restraints were based on the measured distances between paired Gla residues (Gla^{25} and Gla^{30}) involved in the coordination of a single calcium ion in known structures of the calcium-bound human factor IX Gla domain, FIX (1–47) (33, 39). Inclusion of these restraints did not significantly perturb the protein backbone conformation or violate any of the NOE-derived distance constraints involving residues in the N terminus. The 30 conformations with the lowest restraint energy violations were used to represent the structure and the average structure for the ensemble was determined using the Analysis program of InsightII. The Cα trace and backbone heavy atoms of the average structure of calcium-bound glacontryphan-M were superimposed with the average structures of contryphan-R (7), contryphan-Vn (10), and contryphan-Sm (5) using InsightII.

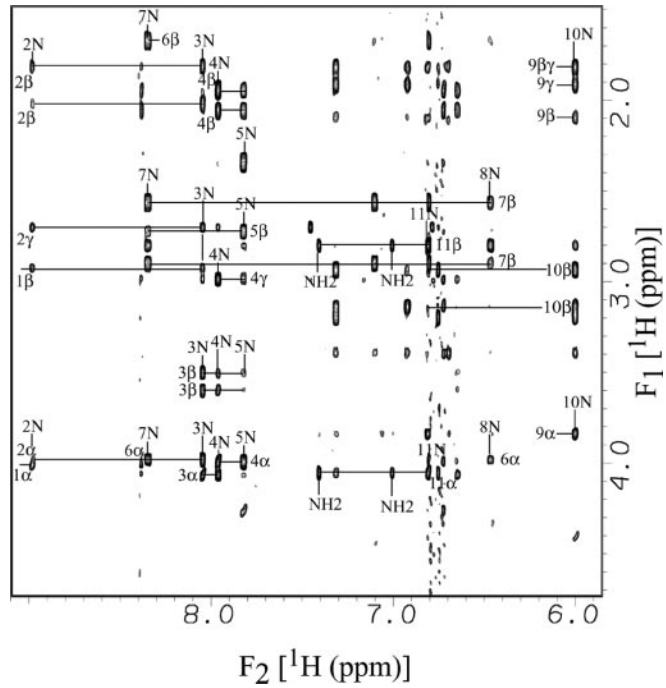

FIG. 1. **Two-dimensional ^{1}H NMR spectral data for metal-free glacontryphan-M.** The annotated amide-α [F_2(NH)-F_1(αH)], fingerprint region (~6.0–9.0 ppm in the F_2 dimension) of a two-dimensional NOESY spectrum of glacontryphan-M in the absence of calcium collected at 9 °C with a mixing time of 400 ms is shown. The intraresidue NH-αH and NH-βH cross-peaks are labeled with the amino acid number. Line connectivities are illustrated between sequential αN(*i*, *i+1*, or *i+2*), βN(*i*, *i+1*, or *i+2*), γN(*i*, *i+1*, or *i+2*) cross-peaks throughout the peptide.

RESULTS

To determine the high resolution structure of glacontryphan-M, a peptide having the mature glacontryphan-M sequence was synthesized with D-tryptophan at position 7, an amidated C terminus, and Gla residues at positions 2 and 4. The primary sequence and the identification of post-translational modifications of native glacontryphan-M (Table I), which was isolated and purified from the venom of *C. marmoreous,* were determined by automated Edman degradation and NanoESI mass spectrometry (11). Following the synthesis and initial purification of glacontryphan-M, the Cys^5-Cys^{11} disulfide bond was formed by oxidative refolding. The HPLC elution profiles of the natural and synthetic glacontryphan-M peptides were identical and when co-injected, the two peptides co-migrated (11).

Determination of the Structure of Glacontryphan-M using Two-dimensional NMR Spectroscopy—The solution structure of glacontryphan-M in the absence of calcium was solved by two-dimensional ^{1}H NMR spectroscopy using NOESY, TOCSY, and DQF-COSY spectra collected at 9 °C and a pH of 5.8. Additional NOESY spectra collected at 35 °C and 15 °C and at 9 °C in fully deuterated solvent permitted the assignment of proton resonances close to the bulk solvent peak and provided additional NOE information. Proton resonances were assigned using sequential connectivities determined by correlating αH and side chain proton connectivities to backbone amide (NH) protons of neighboring residues (28). The annotated "fingerprint" region of a representative NOESY spectrum (Fig. 1) shows the sequential residue αN(*i*, *i*+1) and βN(*i*, *i*+1) connectivities that are observed throughout the peptide in the absence of calcium. In addition, medium and long-range αN(*i*, *i*+n) and βN(*i*, *i*+n) connectivities that define this well structured peptide are included. The proton resonance chemical shifts for metal-free glacontryphan-M are presented in Table II. In contrast to the published results for contryphan-Sm (5), contryphan-R (7), and contryphan-Vn (10), glacontryphan-M is a single homogenous conformer exhibiting no *cis* to *trans* isomerization of the Cys-Pro peptidyl bond in aqueous solution over the temperature range investigated (9–25 °C).

We initially evaluated the glacontryphan-M structure in the absence of calcium by comparing the observed proton and carbon chemical shifts for glacontryphan-M to known random coil chemical shifts for each amino acid (30), adjusted for temperature (Fig. 2). Deviations from these random coil values for the NH proton, αH proton, and Cα carbon backbone chemical shifts provide information on the peptide backbone structure (28, 35) being influenced considerably by neighboring residues when the peptide is structured (36). Several significant upfield (up to

TABLE II
^{1}H chemical shift assignments for glacontryphan-M in the absence or presence of calcium

Residue	Chemical shifts[a]			
	HN	αH	βH	Other
		ppm		
				7.455, 6.783 NH2
Asn[1]		4.020	2.695 (2.671)	(7.440, 6.764)
Gla[2]	8.980 (8.830)	3.981 (4.016)	2.019, 1.811	2.925 (2.914) γH
			3.598, 3.504	
Scr[3]	8.046 (8.146)	4.067 (4.071)	(3.586, 3.500)	
Gla[4]	7.964 (8.164)	3.992 (4.00)	2.050, 1.944	2.988 γH
Cys[5]	7.827	4.266	2.718, 2.343	
Pro[6]		3.981	1.671, 0.944	1.155, 0.221 γH
				2.953, 2.804 δH
D-Trp[7]	8.351 (8.261)	4.454	2.898, 2.562	6.807 δ1H, 9.824 ε1H,
				7.100 ε3H, 7.061ζ2H,
				6.693 ζ3H, 6.826 η2H
His[8]	6.459 (6.479)	4.332	1.073, 0.705	6.725 δ2H
				8.382 ε1H
Pro[9]		3.844	2.105, 1.804	1.909, 1.835 γH
				3.394, 3.136 δH
Trp[10]	6.005	4.403	3.195, 2.925	6.756 δ1H, 10.043 ε1H
				7.315 ε3H, 6.654 ζ2H
				6.920 ζ3H, 6.709η2H
Cys[11]	6.807 (6.887)	4.055	2.800	
NH_2	7.006, 7.407			

[a] Given in absence of calcium (presence of calcium in parentheses) at 9 °C, pH 5.8 in 90% H_2O, 10% D_2O.

2 ppm) chemical shift perturbations are observed for the NH protons of residues His[8], Trp[10], and Cys[11] and for the αH protons of all residues within the intercysteine loop (Cys[5], Pro[6], D-Trp[7], His[8], Pro[9], and Cys[11]) with the exception of Trp[10] (Fig. 2). These results are similar to the random coil chemical shift deviations reported for contryphan-R at 5 °C and pH 5.8 (7). These results suggest that in the absence of calcium, synthetic glacontryphan-M expresses the highly constrained, disulfide-bridged, contryphan loop, which has been observed in previous NMR studies of contryphans-R, Sm, and Vn (5, 7, 10).

NOE connectivities between intraresidue NH protons of the glacontryphan-M peptide backbone and neighboring proton resonances are summarized in Fig. 2 with the strength of each NOE connectivity correlated with bar thickness. The ϕ torsion angles were determined from vicinal $^3J_{HN\alpha}$, coupling constants that were measured in a resolution enhanced DQF-COSY spectrum. Appropriate NH-αH splittings were used to define an allowable range of backbone angle conformations. Where possible the χ^1 rotamers were categorized as 60°, 180°, or −60° by qualitative analysis of β-proton NOE intensities, $d_{\alpha\beta1}$, $d_{\alpha\beta2}$, $d_{N\beta1}$, and $d_{N\beta2}$ (27). Using an initial family of convergent structures to identify a preferred disulfide bond conformation, known distance restraints between the α-carbons of each cysteine residue and between the β-carbon of one cysteine and the sulfur atom of the other cysteine were added (32).

To determine the orientation of the proyl-peptide bonds in glacontryphan-M and to completely resolve ambiguities in the assignment of tryptophan ring proton resonances arising from ^{1}H spectral degeneracy, we collected and assigned a natural abundance ^{1}H-^{13}C HSQC spectrum. Complete ^{13}C carbon resonance assignments for metal-free glacontryphan-M are presented in Table III. Specific regions of the ^{1}H-^{13}C HSQC spectrum are shown in Fig. 3, *A* and *B*, illustrating ^{1}H-^{13}C correlations between the α, β, γ, and δ protons and their directly bonded ^{13}C resonances, and between the aromatic ring protons of both tryptophans as well as histidine and their correlated ^{13}C resonances, respectively. The proyl-peptide bond configuration was determined using the ^{13}C-chemical shift difference between the Cβ and Cγ proline carbons (29, 30). These data identified that the Cys[5]-Pro[6] peptide bond was in the *cis* configuration, while the His[8]-Pro[9] peptide bond was in the

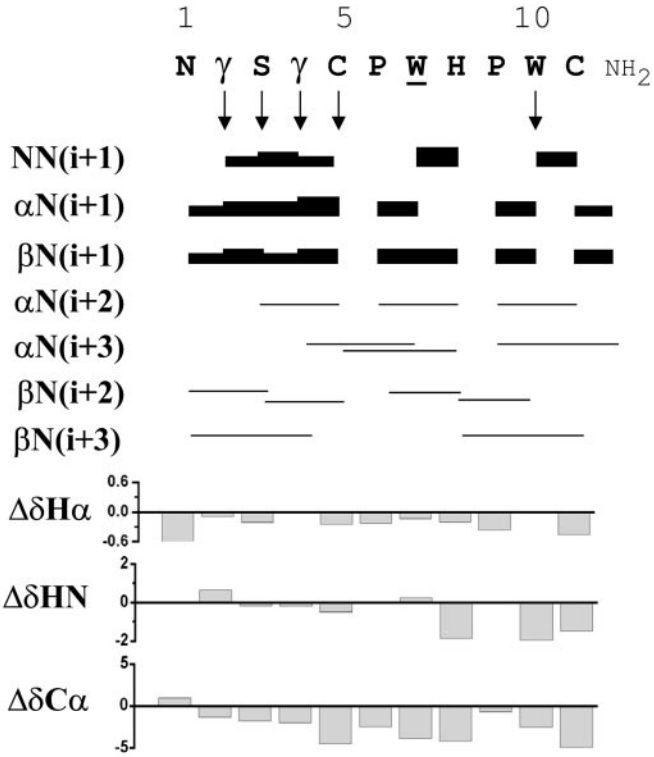

FIG. 2. **Summary of sequential and short to medium range NOE-based connectivities and deviations from random coil chemical shifts.** Summary of NOE data from two-dimensional NOESY spectra collected at pH 5.8 and 9 °C in the absence of calcium. The *thickness* of the *bars* qualitatively represents the intensity of the sequential and NN(*i*, *i+1*), αN(*i*, *i+1*), βN(*i*, *i+1*) NOE connectivities. The rest of the NOE connectivities shown are illustrated with a *connected line*. Plotted below are the deviations of the Hα and HN proton chemical shifts and Cα carbon chemical shifts of glacontryphan-M in the absence of calcium from random coil chemical shift values determined by subtracting the literature random coil shifts from the observed chemical shifts. Residues for which $J^3_{HN\alpha}$ splittings were measured from a two-dimensional COSY spectrum are denoted with an *arrow*; down to indicate a coupling of less than 6.2 Hz.

TABLE III
Natural abundance ^{13}C chemical shift assignments for glacontryphan-M in the absence of calcium

Residue	Chemical shifts[a]			
	Cα	Cβ	Cγ	Others
		ppm		
Asn[1]	54.35	35.70		
Gla[2]	54.93	31.70	55.34	
Ser[3]	57.00	61.64		
Gla[4]	54.18	32.61	55.09	
Cys[5]	51.11	38.76		
Pro[6]	60.57	32.89	21.63	47.88 Cδ
				112.62 Cζ2
D-Trp[7]	53.80	28.93		119.14 Cε3
				122.49 Cη2
				123.15 Cζ3
				125.84 Cδ1
His[8]	52.18	26.55		118.96 Cδ2
				134.80 Cε1
Pro[9]	63.14	29.78	25.53	49.20 Cδ
Trp[10]	55.01	25.12		113.40 Cζ2
				117.64 Cε3
				119.80 Cη2
				121.00 Cζ3
				125.78 Cδ1
Cys[11]	50.78	38.03		

[a] At 9 °C, pH 5.8 in 90% H_2O, 10% D_2O.

trans configuration in the absence of calcium. Critical assessment of the aromatic region of the ^1H-^{13}C HSQC shown in Fig. 3*B* was necessary to ensure that assignments of degenerate tryptophan and histidine ^1H resonances were correct. The restraint file used in simulated annealing and distance geometry calculations for glacontryphan-M in the absence of calcium was comprised of 339 structural restraints (143 intra, 196 inter; 116 sequential, 50 medium, and 30 long range restraints). Following a qualitative analysis of the penultimate family of structures, the χ^3 angle of the disulfide bond (using the previously mentioned known distance restraints) was restrained into the predominantly right-handed configuration (>60°) for calculating the final family of structures.

The Metal-free Structure of Glacontryphan-M Determined by NMR Spectroscopy—Illustrated in Fig. 4 are 35 of the 50 final of convergent structures for glacontryphan-M in the absence of calcium superimposed over the backbone heavy atoms from residues Gla[2] through Trp[10]. The structures are well defined from residues 2 through 11 and are highly convergent with correct stereochemistry. The angular order parameters (S^2) for both ϕ and ψ backbone torsion angles exceed 0.94 for residues Gla[2] through Trp[10]. The RMSD of this ensemble of 35 final structures for the backbone atoms of residues 2–11 is 0.488 Å. The RMSD calculated over the backbone heavy atoms and all heavy atoms, from residues 2–11, respectively, as well as other structural characteristics are summarized in Table IV.

Glacontryphan-M consists of a canonical seven residue contryphan loop that is formed by a disulfide bond between Cys[5] and Cys[11]. The highly constrained looping of the main chain is facilitated in part by the *cis* Cys[5]-Pro[6] peptide bond and D-Trp[7]. Consistent with this, we found oxidation of the Cys[5]-Cys[11] disulfide bond in glacontryphan-M synthesized with L-Trp[7] was problematic due to preferential dimerization (11). A continuum of sequential NOEs between the four N-terminal residues, including the divalent metal ion binding Gla residues, and several NOEs between the side chain Hβ and Hγ protons of Gla4 and the aromatic ring protons of His[8] and Trp[10], respectively, indicate an N-terminal pseudo-turn positioned above the stacked aromatic rings of His[8] and Trp[10]. Aromatic ring stacking between His[8] and Trp[10] shifts the Trp[10] NH resonance significantly upfield and perturbs the His[8] Hβ and ring Hϵ proton resonances. His[8] and Trp[10] are clustered on the same face of the average structure, above the plane formed by the intercysteine loop, while D-Trp[7] lies below. NOEs between Gla[4] and the rings of His[8] and Trp[10] define the structure of the side chain of Gla[4], however, in the absence of calcium both the backbone and side chain resonances of Gla[2] are less ordered.

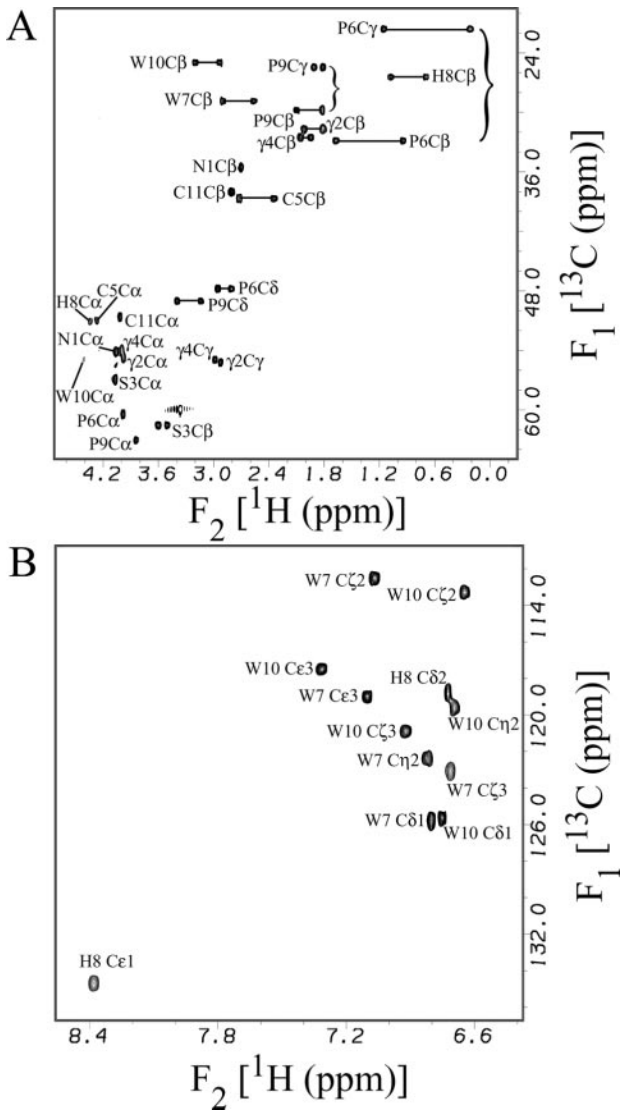

FIG. 3. **Two-dimensional ^1H-^{13}C HSQC NMR spectral data for metal-free glacontryphan-M.** *A*, region from the two-dimensional ^1H-^{13}C HSQC spectrum of metal-free glacontryphan-M acquired at 9 °C with a 2 mM peptide sample at pH 5.8. This region of the spectrum, 20–64 ppm in the F_1 dimension, shows all of the Cα and side chain carbon correlations to protons. The differences between the proline Cβ carbon chemical shifts and Cγ carbon chemical shifts, which are indicated with brackets, were used to determine the *cis* or *trans* orientations of the Cys[5]-Pro[6] and His[8]-Pro[9] peptide bonds in glacontryphan-M. The assignments of the ^1H-^{13}C cross-peaks are annotated and the ^{13}C chemical shifts are listed in Table III. *B*, region from the same two-dimensional ^1H-^{13}C HSQC spectrum of metal-free glacontryphan-M shown in *A* that contains the aromatic side chain carbon to proton correlation cross-peaks of D-Trp[7], His[8], and Trp[10], ~112–136 ppm in the F_1 dimension. The assignments of the ^1H-^{13}C cross-peaks are annotated, and the ^{13}C chemical shifts are listed in Table III.

Calcium Ion Binding of Glacontryphan-M: Circular Dichroism and NMR Spectroscopy—Calcium-induced quenching of the intrinsic fluorescence of glacontryphan-M has been observed (11). These fluorescence data showed a single, saturable calcium binding site with a K_D of 0.63 mM. To determine the influence of calcium binding on the structure of glacontryphan-M, we first used circular dichroism (CD) in the near UV wavelength range to observe the absorbance transitions of the

aromatic amino acid side chains, specifically ring flipping perturbations of D-Trp[7] and Trp[10], and changes in the disulfide bond angle χ^3 chirality (37). The CD spectra observed in the absence and presence of calcium are essentially superimposable suggesting that calcium binding to glacontryphan-M does not induce major structural alterations (Fig. 5*A*). The positive absorbance band at ~260 nm that is seen over the strong negative tryptophan absorbance bands can be attributed to the chirality of the disulfide bond (37). For a disulfide χ^3 angle of less than 90°, a positive absorbance band at ~260 nm confirms a right-handed disulfide orientation in the determined glacontryphan-M structure. The disulfide χ^3 angle remains in right-handed configuration in the presence of calcium. No further differences in the CD spectra were seen at 30 molar equivalents of calcium (data not shown). The lack of significant structural transition suggests that the observed calcium-induced fluorescence quenching of glacontryphan-M is the result of localized-structural perturbations.

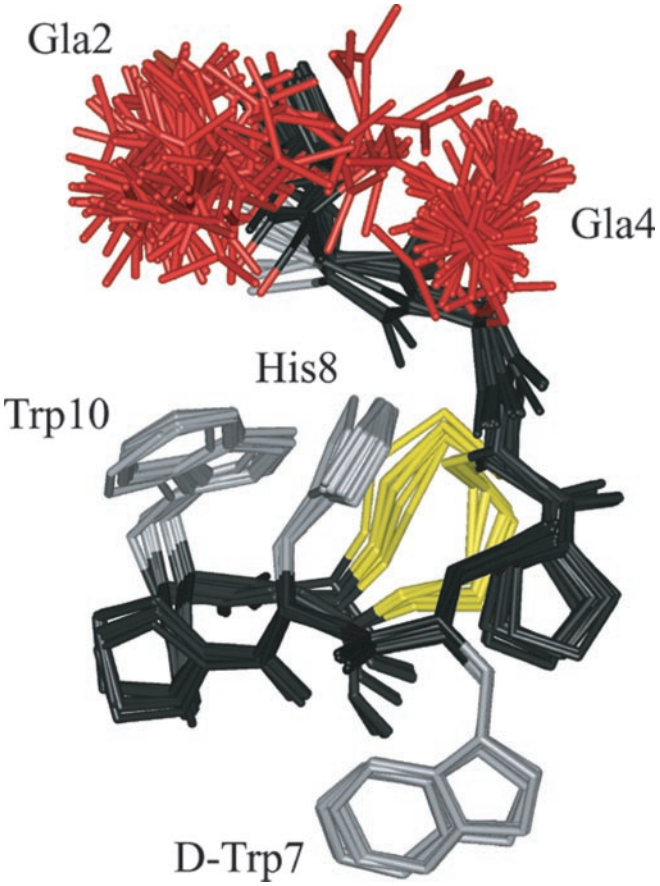

FIG. 4. **The family of low energy conformations of metal-free glacontryphan-M.** This family of 35 structures of metal-free glacontryphan-M was determined from distance geometry calculations. Individual structures have been superimposed over the backbone N, C, and Cα atoms of residues 4–11; and residues 2–11 are shown. The backbone is rendered in *black*, the disulfide bond in *yellow*, the side chains of Gla[2] and Gla[4] in *red*, and the side chains of Ser[3], D-Trp[7], His[8], and Trp[10] in *gray*.

Two-dimensional TOCSY and NOESY data obtained for glacontryphan-M in the presence of 15 molar equivalents of calcium showed specific backbone amide (NH) proton and Hα proton as well as side chain proton chemical shift perturbations. Fifteen molar equivalents of calcium was near saturating since at higher calcium:peptide ratios (60:1) only trace additional chemical shift perturbations were observed (data not shown), consistent with the CD data described above. The absolute value of NH chemical shift changes were determined from TOCSY spectra for glacontryphan-M in the absence and presence of calcium and are shown in Fig. 5*B*. The largest NH chemical shift perturbations were observed for Gla[2], Ser[3], and Gla[4], consistent with calcium binding by the malonate-like side chains of Gla[2] and Gla[4]. Examinations of calcium-induced perturbations of ^{13}C resonances in natural abundance ^{1}H-^{13}C HSQC spectra (data not shown) confirmed the specificity of calcium interaction in the N terminus and the localization of calcium-induced perturbations. Altering the pH or temperature did not perturb the ^{1}H or ^{13}C chemical shifts of glacontryphan-M in the presence of calcium with the exception of the His[8] ring proton, Hϵ. However, at pH 7.0, we observed significant loss of NOE data as a result of solvent exchange that remained at reduced temperatures (data not shown).

The Calcium-bound Structure of Glacontryphan-M Determined using NMR Spectroscopy—To determine the calcium-bound structure of glacontryphan-M and to identify critical functional determinants, two-dimensional NOESY, TOCSY, and DQF-COSY spectra of the glacontryphan-M in the presence of 15 molar equivalents of calcium were collected. All of the proton resonances were assigned as described for the metal-free glacontryphan-M structure determination. The main chain proton (HN and αH) resonance chemical shifts for calcium-bound glacontryphan-M are presented in parentheses in Table II. As for the metal-free conformer, glacontryphan-M in the presence of calcium is represented by a single conformer with no isomerization of the Cys-Pro peptidyl bond observed over the temperature range studied. A final family of 50 convergent structures was calculated from the NOE-based restraints. Thirty representative structures from the final family of 50 calculated structures are shown in Fig. 6, superimposed over the backbone heavy atoms from residues Gla[2] to Trp[10]. The mean RMSD calculated over the backbone heavy atoms and all heavy atoms, from residues 2–11, respectively, as well as other structural characteristics are summarized in Table IV. The angular order parameters (S^2) for both ϕ and ψ backbone torsion angles exceed 0.93 for residues Gla[4] through Cys[11]. The RMSD to the calculated geometric average structure for the

TABLE IV
Statistics for glacontryphan-M NMR structures in the absence and presence of calcium

	Glacontryphan-M in the absence of calcium	Glacontryphan-M in the presence of calcium
No. of residues giving NOEs	11	11
Total NOE-based restraints	339	288
NOE-based restraints/residue	30.8	26.2
Additional distance restraints	7	9
Torsion angle restraints	30	12
Calcium ligand restraints	0	6
RMSD relative to average structure		
Residues 2–11 backbone atoms (Å)	0.356	0.538
Residues 2–11 all atoms (Å)	0.953	1.312
Residues 5–11 backbone atoms (Å)	0.368	0.207
Residues 5–11 all atoms (Å)	0.638	0.585

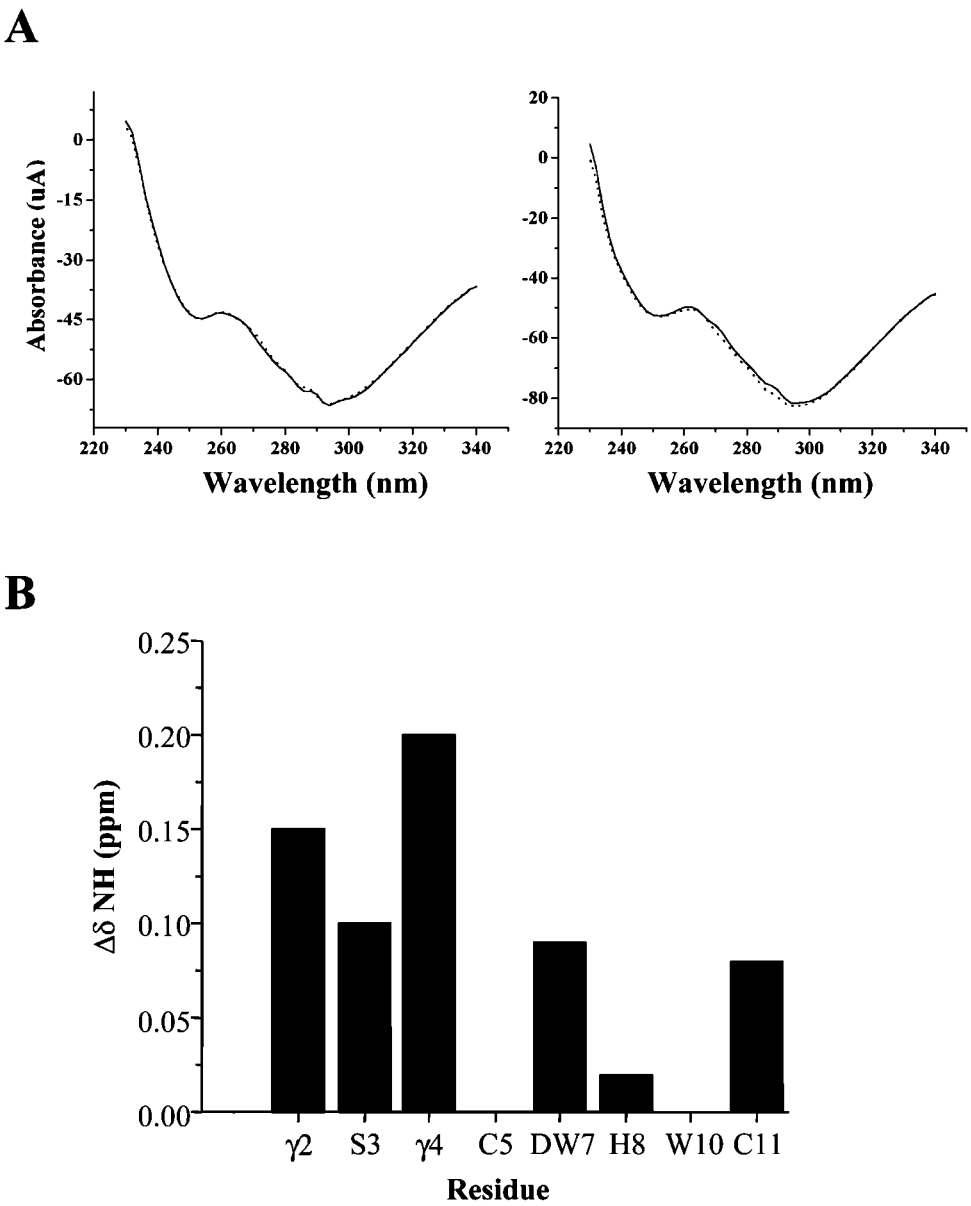

FIG. 5. **Perturbation of glacontryphan-M induced upon calcium ion binding.** *A*, circular dichroism spectrum in the near-UV wavelength range of glacontryphan-M (0.20 mM) in H_2O at 25 °C in the absence (*solid*) and presence of 15 molar equivalents of calcium (*dashed line*), at pH 5.8 on the *left* and pH 7.0 on the *right*. Spectra were recorded from 340 to 230 nm and represent the average of three scans acquired with a dwell time of 3 s/nm. The data are expressed in terms of units of absorbance. *B*, chemical shift perturbations observed in two-dimensional TOCSY spectrum of glacontryphan-M at pH 5.8 as a function of calcium ion binding are indicated by the absolute value of the NH chemical shift perturbations for all resonances, except the prolines, of glacontryphan-M in the presence of 15 molar equivalents of calcium at 9 °C. Δδ NH, $|\delta_{NH(Ca^{2+})} - \delta_{NH(Apo)}|$.

well-defined backbone residues of 2–11 in the 30 final structures is 0.538 Å.

Comparison of the Metal-free and Calcium-bound Glacontryphan-M Structures—To fully appreciate the calcium-induced structural perturbations of glacontryphan-M, we superimposed the average metal-free (black) and calcium-bound (red) glacontryphan-M structures (Fig. 7*A*) using the backbone atoms of Cys^5 through Cys^{11}. It is apparent that calcium ion binding alters the structure of glacontryphan-M in the N-terminal region. In the absence of calcium, Asn^1, Gla^2, Ser^3, and Gla4 form a pseudoturn positioned above His^8 and Trp^{10}. Following calcium binding, the backbone atoms of Gla^2 and Ser^3 are reoriented, bringing Gla^2 closer to Gla^4. In addition, the N terminus is in a more extended conformation that is approximately perpendicular to the plane of the intercysteine loop and further from Trp^{10} resulting in greater exposure of the side chains of His^8 and Trp^{10}.

To further demonstrate specific calcium-induced perturbations within the N terminus, the average per residue coordinate precision for the backbone heavy atoms of the metal-free and calcium-bound families of glacontryphan-M structures were determined (InsightII). The average coordinate precision for all structures in the final metal-free and calcium-bound families was used to render the respective peptide backbones as sausage ribbons (Fig. 7*B*). The radii of the sausage ribbons are representative of the backbone heavy atom coordinate precision for each residue. Fig. 7*B* illustrates the significant coordinate precision for the metal-free (black) and calcium-bound (red) conformers of glacontryphan-M permitting the calcium-induced perturbations that are localized around the N-terminal residues to be clearly observed. The superimposition of the atomic coordinate precision along the backbone of the intercysteine loop residues, Pro^6 through Trp^{10}, indicates that structural differences between the backbones of the metal-free

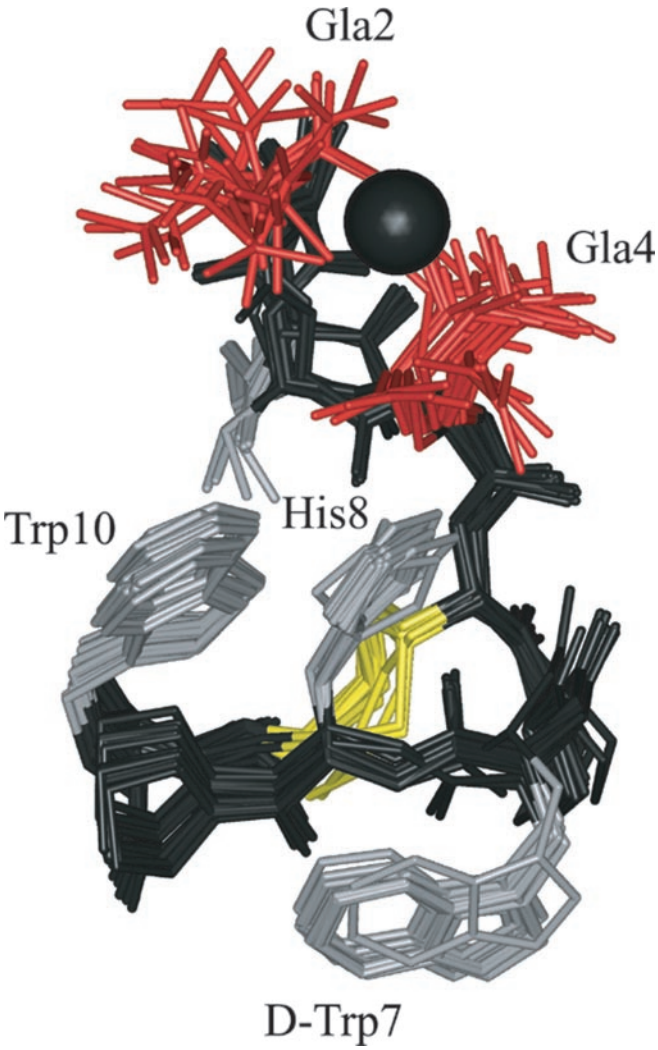

FIG. 6. **The family of low energy conformations of glacontryphan-M in the presence of calcium.** This family of 30 structures was determined from distance geometry calculations. Individual structures have been superimposed over the backbone N, C, and Cα atoms of residues 4–11; and residues 2–11 are shown. The backbone is rendered in *black*, the disulfide bond in *yellow*, and the side chains of Gla^2 and Gla^4 in *red*, and the side chains of Ser^3, D-Trp^7, His^8, and Trp^{10} in *gray*. The *black sphere* represents a bound calcium ion.

(black) and calcium-bound (red) structures of glacontryphan-M in this region are not significant.

In addition to these N-terminal perturbations, the intercysteine disulfide loop, Cys^5-Cys^{11}, is altered which positions the disulfide bridge closer to the loop interior, while maintaining the same χ3 angle (Fig. 7, *A* and *B*). The D-Trp^7 and His^8 side chains are slightly reoriented in the presence of calcium with respect to the positioning of the Trp^{10} ring. The D-Trp^7 side chain is oriented closer to the intercysteine loop backbone and closer to the stacked aromatic rings of His^8 and Trp^{10}. In addition to the Gla and aromatic amino acids, the side chain -OH of Ser^3 is positioned closer to the aromatic ring of Trp^{10}. The alterations in structure that accompany calcium binding to glacontryphan-M, especially the rearrangement occurring around the two tryptophan residues and/or the disulfide bridge, help explain the observed quench of the intrinsic glacontryphan-M fluorescence by calcium binding.

DISCUSSION

We have determined the metal-free and calcium-bound high resolution structures of a novel Gla-containing *Conus* peptide, glacontryphan-M. A comparison of the two structures reveals subtle calcium-induced perturbations that reposition the Gla-containing N-terminal residues that are unique to glacontryphan-M. These calcium-induced perturbations result in increased exposure of the stacked aromatic rings of His^8 and Trp^{10}, perturbation of the Cys^{11}-Cys^5-Pro^6 intercysteine loop region, and altered alignment of the His^8 and D-Trp^7 aromatic rings with respect to that of Trp^{10}. These structural data provide several mechanistic explanations for the observed calcium-dependent intrinsic fluorescence quench of glacontryphan-M (11). In addition, these structures reveal calcium interactions with glacontryphan-M that are required for the block of voltage-gated L-type Ca^{2+} channels.

Glacontryphan-M is the first contryphan shown to antagonize voltage-gated calcium channels and the first found containing Gla residues (11). Our structure of glacontryphan-M contains the canonical contryphan fold demonstrating that the scaffold (CP*(D-W or D-L)*X*PWC) is robust with respect to a histidine substitution at the variable position, *X*. Attempts to fold glacontryphan-M synthesized with L-Trp^7 failed due to the exclusive formation of peptide dimers, lending support to the structural necessity of D-Trp^7. *In vivo* D-amino acids are reported to increase peptide bond stability and decrease proteolytic degradation (38). The D-Trp-containing contryphans characterized to date demonstrate greater biological activity than their D-Leu-containing family members in eliciting stiff-tail syndrome and paralysis of extremities in mice (9). This finding suggests that either the D-handed residue plays a role in the biological activity of contryphans, or the aromatic ring stacking of the D-Trp^7 and Trp^{10} side chains in the D-Trp-containing contryphans results in enhanced function or increased peptide stability.

Among the contryphans, substitution at other positions within the intercysteine loop only modestly perturbs the backbone conformation suggesting some conformational flexibility within this loop (10). Contryphans characterized to date are a mixture of two conformers in solution due to *cis-trans* isomerization of the N-terminal Cys-Pro peptide bond (5). In contrast to previous structure/function studies of contryphan-Sm in which the *cis-trans* ratio of the Cys-Pro peptide bond was shown to be dependent on stabilizing electrostatic interactions between an N-terminal glycine residue and a glutamine that is positioned between D-Trp and Pro^9 (5), we observed no isomerization in glacontryphan-M in the absence or presence of calcium. Others have asserted that isomerization of the Cys-Pro peptide bond is driven by hydroxylation of the proline in combination with the adjacent D-handed tryptophan (4). Our data indicate that the lack of isomerization in glacontryphan-M is attributable in part to decreased structural mobility of the intercysteine loop as indicated by NOE contacts between the N-terminal cluster of residues that include Gla and the aromatic rings of His^8 and Trp^{10}, as well as numerous NOE contacts from Pro^6 and Pro^9 to neighboring residues in the intercysteine loop.

This structural investigation suggests that the function for Gla in voltage-gated Ca^{2+} channel blockage by glacontryphan-M is one of the following: 1) to alter the structure of glacontryphan-M such that a calcium-dependent conformational perturbation results in the presentation of functional determinants that interact with the channel; 2) to enable glacontryphan-M to bind to the membrane surface through calcium bridging of Gla residues and membrane components for interaction with specific calcium channel sites; or 3) to ensure that there is a localized enrichment of calcium ions at the channel opening, that might facilitate a change in the structure of the channel allowing glacontryphan-M to bind to a higher affinity antagonist binding site. There is precedent for the

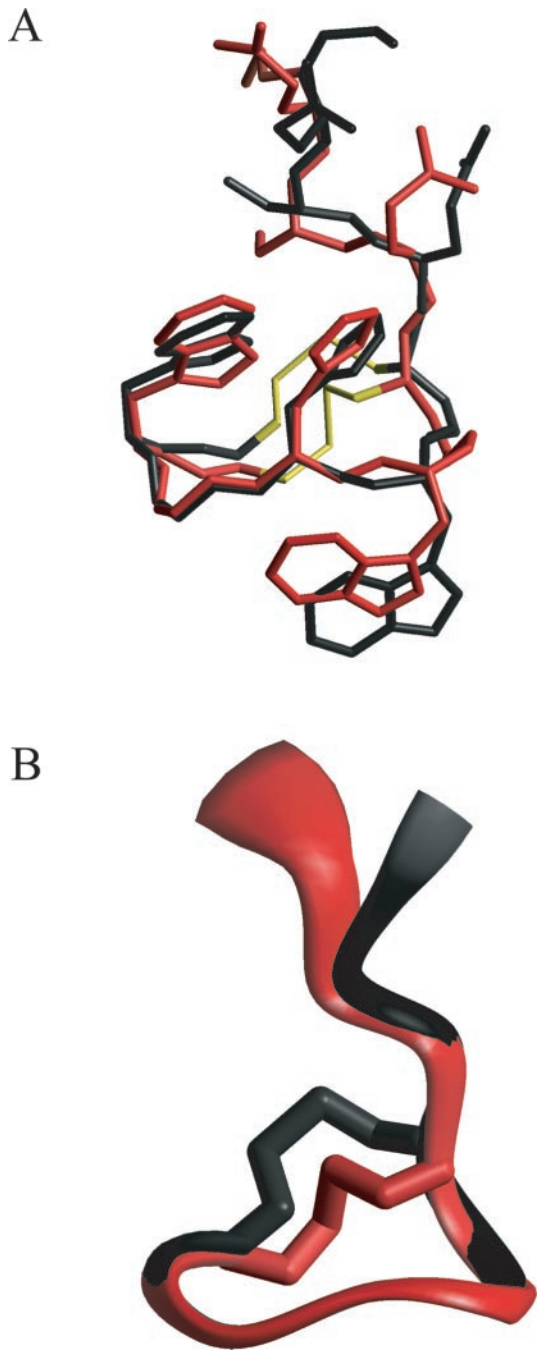

FIG. 7. **Comparison of the average metal-free and calcium-bound glacontryphan-M conformations.** *A*, average structures of metal-free (*black backbone*) and calcium-bound (*red backbone*) glacontryphan-M are shown superimposed across the backbone N, C, and Cα atoms of all of the intercysteine loop residues, Cys^5, Pro^6, D-Trp^7, His^8, Pro^9, Trp^{10}, Cys^{11}. *B*, peptide backbones of the superimposed metal-free (*black*) and calcium-bound (*red*) glacontryphan-M structures are presented using variable width *ribbons* rendered as *sausages*. The radius of each ribbon represents the calcu-lated backbone heavy atom coordinate precision determined for each residue over all structures of the final metal-free and calcium-bound families, respectively.

modulation of antagonist affinities by calcium binding to L-type Ca^{2+} channels. Voltage-gated L-type Ca^{2+} channel antagonists, in particular the 1,4-dihydropyridine (DHP) class of antagonists, bind to a higher affinity class of sites on the Ca^{2+} channel when the channel itself is calcium bound (15). While the mechanism through which this class of antagonists functions is poorly understood, it is known that in the absence of calcium, these DHP antagonists bind to lower affinity sites on the channel.

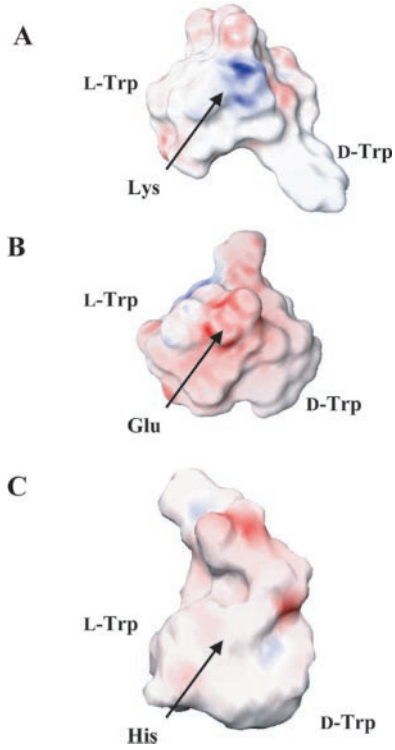

FIG. 8. **Surface view of the electrostatic potentials of the related contryphans: contryphan-Vn, contryphan-R and glacontryphan-M.** The structures of contryphan-Vn and contryphan-R have been previously determined using two-dimensional homonuclear NMR spectroscopy (7, 8). The average structures of contryphan-Vn (*A*), contryphan-R (*B*), and glacontryphan-M (*C*) are shown with surface filling electrostatic maps that were determined using GRASP software (34). The surfaces of the molecules are colored according to their electrostatic potential maps, scaled from electronegative (*red*) to electropositive (*blue*). The variable residue between the D-Trp and Pro, L-Trp residues of the intercysteine loop in each contryphan are labeled.

A comparison of the known contryphan three-dimensional structures (Table I) provides a first step toward structure-function studies as these contryphans share high sequence similarity, yet have unique N-terminal sequences and a variable residue positioned between D-Trp and the C-terminal Pro. Contryphan-Vn is a D-Trp-containing contryphan isolated from *Conus ventricosus* (10) with a positively charged Lys residue within the intercysteine loop. The presence of the intercysteine lysine and an N-terminal Asp residue confer a distinct surface electrostatic potential to contryphan-Vn (Fig. 8) where most of the charged surface is characterized by two opposing potential values: positive from the intercysteine lysine and negative from the N-terminal aspartate. In contrast to contryphan-Vn, electrostatic potential calculations of contryphan-R, a D-Trp-containing contryphan isolated from *Conus radiatus* (7), yield a surface charge distribution mostly characterized by an acidic charge potential (Fig. 8). The variable residue in contryphan-R is Glu. The presence of the intercysteine histidine in glacontryphan-M yields a surface charge distribution characterized by a large, neutral charge potential surface patch of the intercysteine loop hydrophobic residues D-Trp^7, His^8, Pro^9, and Trp^{10}, and an acidic N terminus comprised of the two Gla residues at positions 2 and 4 (Fig. 8). Calcium ions were not added in the electrostatic potential calculations, but presumably the charge of the acidic Gla residues is partially neutralized by a chelated calcium ion in glacontryphan-M. These results suggest that the determinants that underlie molecular recognition of glacontryphan-M are unique from those of the other known contryphans. A complete understanding of the structure-function relationships in the contryphan family, especially the pharmacological

activity that is attributed to the triad of hydrophobic residues (D-Trp, His, and Trp) in glacontryphan-M, may lead to the development of novel neuropharmacological reagents.

REFERENCES

1. Espiritu, D. J. D., Watkins, M., Dia-Monje, V., Cartier, G. E., Cruz, L. J., and Olivera, B. M. (2001) *Toxicon* **39,** 1899–1916
2. Jimenez, E. C., Craig, A. G., Watkins, M., Hillyard, D. R., Gray, W. R., Gulyas, J., Rivier, J. E., Cruz, L. J., and Olivera, B. M. (1997) *Biochemistry* **36,** 989–994
3. Jimenez, E. C., Olivera, B. M., Gray, W. R., and Cruz, L. J. (1996) *J. Biol. Chem.* **271,** 28002–28005
4. Jacobsen, R. B., Jimenez, E. C., De la Cruz, R. G. C., Gray, W. R., Cruz, L. J., and Olivera, B. M. (1999) *J. Peptide Res.* **54,** 93–99
5. Pallaghy, P. K., He, W., Jimenez, E. C., Olivera, B. M., and Norton, R. S. (2000) *Biochemistry* **39,** 12845–12852
6. Pallaghy, P. K., and Norton, R. S. (2000) *Biopolymers* **54,** 173–179
7. Pallaghy, P. K., Melnikova, A. P., Jimenez, E. C., Olivera, B. M., and Norton, R. S. (1999) *Biochemistry* **28,** 11553–11559
8. Massilia, G. R., Schinina, M. E., Ascenzi, P., and Polticelli, F. (2001) *Biochem. Biophys. Res. Commun.* **288,** 908–913
9. Jimenez, E. C., Watkins, M., Juszczak, L. J., Cruz, L. J., and Olivera, B. M. (2001) *Toxicon* **39,** 803–808
10. Massilia, G. R., Eliseo, T., Grolleau, F., Lapied, B., Barbier, J., Bournaud, R., Molgo, J., Cicero, D. O., Paci, M., Schinina, M. E., Ascenzi, P., and Polticelli, F. (2003) *Biochem. Biophys. Res. Commun.* **303,** 238–246
11. Hansson, K., Ma, X., Eliasson, L., Czerwiec, E., Furie, B., Furie, B. C., Rorsman, P., and Stenflo, J. (2003) *J. Biol. Chem.* **279,** 32453–32463
12. McIntosh, J. M., Olivera, B. M., Cruz, L. J., and Gray, W. R. (1984) *J. Biol. Chem.* **259,** 14343–14346
13. Haack, J. A., Rivier, J., Parks, T. N., Mena, E. E., Cruz, L. J., and Olivera, B. M. (1990) *J. Biol. Chem.* **265,** 6025–6029
14. Nakamura, T., Yu, Z., Fainzilber, M., and Burlingame, A. L. (1996) *Protein Sci.* **5,** 524–530
15. Mitterdorfer, J., Grabner, M., Kraus, R. L., Hering, S., Prinz, H., Glossmann, H., and Striessnig, J. (1998) *J. Bioenerget. Biomembr.* **30,** 319–334
16. Rigby, A. C., Baleja, J. D., Li, L., Pedersen, L. G., Furie, B. C., and Furie, B. (1997) *Biochemistry* **36,** 15677–15684
17. Skjaerbaek, N., Nielsen, K. J., Lewis, J., Alewood, P., and Craik, D. J. (1997) *J. Biol. Chem.* **272,** 2291–2299
18. Blandl, T., Warder, S. E., Prorok, M., and Castellino, F. J. (1999) *J. Peptide. Res.* **53,** 453–464
19. Furie, B., and Furie, B. C. (1988) *Cell* **53,** 505–518
20. Stenflo, J., and Dahlback, B. (2001) in *The Molecular Basis of Blood Disease* (Stamatoyannopoulus, G., Majerus, P.W., Perlmutter, R. M., and Varmus, H., eds) pp. 579–613, WB Saunders, New York
21. Sunnerhagen, M., Forsen, S., Hoffren, A.-M., Drakenberg, T., Teleman, O., and Stenflo, J. (1995) *Nat. Struct. Biol.* **2,** 504–509
22. Freedman, S. J., Blostein, M. D, Baleja, J. D., Jacobs, M., Furie, B. C., and Furie, B. (1996) *J. Biol. Chem.* **271,** 16227–16236
23. Huang, M., Rigby, A. C., Morelli, X., Grant, M. A., Huang, G., Furie, B., Seaton, B., and Furie, B. C. (2003) *Nat. Struct. Biol.* **10,** 751–756
24. Pain, R. (1996) *Protocols in Protein Science*, pp. 7.6.1–7.6.23, John Wiley & Sons, Inc., New York
25. Bax, A., and Davis, D. G. (1985) *J. Magn. Reson.* **65,** 355–360
26. Clore, G. M., and Gronenborn, A. M. (1989) *Crit. Rev. Biochem. Mol. Biol.* **24,** 479–564
27. Barsukov, I. L., and Lian, L.-Y. (1993) in *NMR of Macromolecules: A Practical Approach* (Roberts, G. C. K., ed) pp. 315–357, Oxford University Press, Oxford
28. Wuthrich, K. (1986) *NMR of Proteins and Nucleic Acids*, pp. 130–199, John Wiley & Sons, Inc., New York
29. Richarz, R., and Wurthrich, K. (1978) *Biopolymers* **17,** 2133–2141
30. Schwarzinger, S., Kroon, G. J. A., Foss, T. R., Wright, P. E., and Dyson, H. J. (2000) *J. Biomol. NMR* **18,** 43–48
31. Havel, T. F. (1991) *Prog. Biophys. Mol. Biol.* **56,** 43–78
32. Richardson, J. S. (1981) *Adv. Prot. Chem.* **34,** 167–339
33. Freedman, S. J., Furie, B. C., Furie, B., and Baleja, J. D. (1995) *Biochemistry* **34,** 12126–12137
34. Nicholls, A., Sharp, K. A., and Honig, B. (1991) *Proteins* **11,** 281–296
35. Pastore, A., and Saudek, V. (1990) *J. Magn. Reson.* **90,** 165–176
36. Wishart, D. S., Bigam, C. G., Holm, A., Hodges, R. S., and Sykes, B. D. (1995) *J. Biomol. NMR* **5,** 67–81
37. Woody, R. W., and Dunker, A.K. (1996) in *Circular Dichroism and the Conformational Analysis of Biomolecules* (Fasman, G. D., ed) pp. 109–157, Plenum Press, New York
38. Kreil, G. (1997) *Annu. Rev. Biochem.* **66,** 337–345
39. Huang, M., Furie, B. C., and Furie, B. (2004) *J. Biol. Chem.* **279,** 14338–14346

The Metal-free and Calcium-bound Structures of a γ-Carboxyglutamic Acid-containing Contryphan from *Conus marmoreus*, Glacontryphan-M

Marianne A. Grant, Karin Hansson, Barbara C. Furie, Bruce Furie, Johan Stenflo and Alan C. Rigby

J. Biol. Chem. 2004, 279:32464-32473.
doi: 10.1074/jbc.M313826200 originally published online May 20, 2004
